JGR Space Physics

RESEARCH ARTICLE
10.1029/2019JA027536

Ionospheric *D* Region Parameters Obtained Using VLF Measurements in the South Pacific Region

Abhikesh Kumar[1] and Sushil Kumar[1]

[1]School of Engineering and Physics, The University of the South Pacific, Suva, Fiji

Key Points:
- 1.Ionospheric *D* region Wait parameters (H' and β) are determined using Long Wave Propagation Code for both day and nighttime paths
- 2.The nighttime variability showed H' and β between 83.9 - 84.4 km and 0.60 - 0.68 km^{-1}, respectively
- 3.The day-to-day variability at midnight showed H' and β between 83.0 - 85.2 km and 0.58 - 0.82 km^{-1}, respectively

Correspondence to:
A. Kumar,
kumar_ab@usp.ac.fj

Citation:
Kumar, A., & Kumar, S. (2020). Ionospheric *D* region parameters obtained using VLF measurements in the South Pacific region. *Journal of Geophysical Research: Space Physics*, *125*, e2019JA027536. https://doi.org/10.1029/2019JA027536

Received 17 OCT 2019
Accepted 12 DEC 2019
Accepted article online 20 DEC 2019

Abstract The diurnal variations in the phase and amplitude of very low frequency (VLF) transmissions with the call signs NWC, NPM, and NLK, received at Suva, Fiji, have been modeled using the Long Wave Propagation Capability (V2.1) code to determine the ionospheric *D* region parameters, H' (reference height), and β (rate of increase of electron density with height), for different daytime and nighttime conditions along the transmitter-receiver great circle paths (TRGCPs). Measured VLF signal amplitude and phase show explicit variation over the day and nighttime along a TRGCP, also revealing amplitude minima and phase steps during sunrise and sunset as the day/night terminator traverses a TRGCP. While the daytime signal strength is reasonably smooth, at nighttime, the signal exhibits a great deal of variability. For three signal paths, the mean daytime H' and β were found to be 70.7 km and 0.40 km^{-1}, respectively, while nighttime mean values of these parameters were found to be 84.2 km and 0.68 km^{-1}, respectively. The temporal and day-to-day variability of the nighttime *D* region parameters shows that H' and β ranges in between 83.0 and 85.0 km and 0.58 and 0.80 km^{-1}, respectively. One of the possible sources of nighttime signal variability is increase in the number of modes propagating and relative complex interference between them along the TRGCPs, whereby the weaker modes also become significant at night due to reduced attenuation. In addition, the variations in the nighttime D region may also be a cause of high signal variability.

1. Introduction

The amplitude and phase of very low frequency (VLF) signals radiated from navigational transmitters received at any point on Earth generally depend on the state of the lower ionosphere and the electrical parameters of Earth along the propagation path. In addition, the observed signals also vary depending on the time of day, transmitter-receiver great circle path (TRGCP) length, path orientation, magnetic latitude, and the frequency of the VLF transmission. At VLF, the lower region of the ionosphere and the Earth's surface act as good electrical conductors having sufficient conductivities to reflect these waves when incident upon the boundaries. VLF signals propagate long distances via waveguide effects in the Earth-ionosphere waveguide (EIWG) with very little attenuation (1–2 dB/Mm) (Wait, 1962). The conductivity of the Earth (ground or sea parts separately) is assumed to remain constant for a fixed TRGCP. However, the variation in the conductivity of the lower ionosphere due to variable solar radiation leads to the changes in the observed amplitude and phase of VLF signals. As the signals propagate long distances along the east-west meridian, varying solar radiations are encountered. The signals propagating from the transmitter when it is in daylight portion may reach the receiver when it is in dark or vice versa due to transition of the day-night terminator. The VLF signals on emerging from terminator show fadings in the amplitude (minima) and step changes in the phase at any receiving station, which are more apparent over paths with significant component in east-west directions (Clilverd et al., 1999; Crombie, 1964; Ries, 1967).

VLF radio waves can enter some distance into seawater due to their skin effect, which allows for VLF subsurface seawater propagation. Several countries still operate a number of powerful VLF navigational transmitters to communicate with their submarines because VLF signals can be readily detected after propagating long distances of thousands of kilometer. The amplitude and phase of the received VLF signals can provide a good measure of the Wait and Spies parameters, *D* region reference height (H'), and sharpness of the lower edge (β) of the *D* region (Wait & Spies, 1964). The US Naval Ocean Systems Center (NOSC) developed computer programs such as MODESRCH (modesearch), MODEFNDR (modefinder), and Long Wavelength Propagation Capability (LWPC) e.g., (Ferguson & Snyder, 1990; Morfitt & Shellman, 1976) which can be used to investigate the *D* region ionosphere for H' and β.

Daytime propagation is found to be fairly stable, consequently resulting in distinct values of H' and β characterizing the lower D region. NOSC suggested $H' = 70$ km and $\beta = 0.5$ km^{-1} for summer midlatitudes (by implication low latitudes) but $H' = 72$–75 km and $\beta = 0.3$ km^{-1} for winter midlatitudes (Comité Consultatif International des Radiocommunications, 1990; Morfitt, 1977). Amplitude measurements were only used to derive these parameters, mainly versus distance from aircraft journeys lasting for several hours. No inclusion was taken of the changes in H' and β with solar zenith angle variation during the day. The changes in H' and β by means of solar zenith angle were later measured and described by Thomson (1993) and McRae and Thomson (2000) by measuring amplitude and relative phase changes at fixed locations during selected days. These authors obtained $H' = 70$ km for summer midday of solar maximum, by measuring the amplitude at a particular location near a modal minimum at a range of ~600 km over a midlatitude, on a mixture of land and sea path (Thomson, 1993). NOSC obtained a value of $H' = 70$ km for summer midday from the positions of the amplitude modal minima on flights at the times that the aircraft traveled through them. The values of β were actually determined from the attenuation for the paths, assumed constant along the paths for NOSC, and assumed to be changing with solar zenith angle for Thomson (1993) and McRae and Thomson (2000).

Thomson et al. (2007) determined the nighttime D region ionospheric parameters using a wide set of VLF phase and amplitude measurements. They made VLF measurements with several frequencies in the range 10–41 kHz on long, mostly all sea-based paths, including Omega La Reunion and Omega Argentina to Dunedin, New Zealand, NAA (Maine, USA) and NAU (Puerto Rico) to Cambridge, UK, and NPM to San Francisco. The average values of H' and β over many days, for the midlatitude D region near solar minimum were found to be 85.1 $\pm$ 0.4 km and 0.63 $\pm$ 0.04 km^{-1}, respectively. Furthermore, Thomson (2010) was able to improve the values of ionospheric parameters for the lower D region using observed phase and amplitude of VLF signals propagating on a short (~300 km) path from NWC to Karratha/Dampier on the Australian NW coast. The lower edge of the midday equatorial ionosphere was found to be having $H' = 70.5 \pm 0.5$ km and $\beta = 0.47 \pm 0.03$ km^{-1}. According to Thomson (2010), the short path amplitude and phase provided a better accuracy for D region parameters without having to average along the very long paths. Thomson et al. (2011) from the short (300 km) NWC-Karratha and NWC-Dampier paths estimated the midday values of H′ = 69.7 + 0.4 km and β = 0.48 + 0.03 km−1. More recently, Thomson et al. (2014) using the amplitude and phase measurements from NPM for a short, mostly sea-based path between two Islands of Hawaii, determined H' and β of the daytime D region as a function of solar zenith angle (SZA). The H' and β were found to vary from $H' = 69.3 \pm 0.3$ km and $\beta = 0.49 \pm 0.02$ km^{-1} for SZA ~10° at midday, to $H' > 80$ km and β ~0.30 km^{-1} as the SZA approached ~70°–90° near dawn and dusk for this path. The broadband signals generated from lightning discharges have been successfully used for the remote sensing of the D region (e.g., Cheng et al., 2006; Cummer et al., 1998; Han et al., 2011; Han & Cummer, 2010a). Han and Cummer (2010a) determined the midlatitude daytime ionospheric D region electron density profile using ELF-VLF atmospherics recorded at Duke University, USA. Their results showed that the temporal variations in the daytime D region electron density profile are quantitatively related to changes in solar zenith angles. The quiet time D region reference height reduced from ~80 km near sunrise to ~71 km near noon when the solar zenith angle was minimum.

The VLF propagation in the EIWG is very sensitive to the D region conditions along any TRGCP. Therefore, any disturbance in the D region appears as a perturbation in the recorded VLF signal (amplitude and phase) at the receiver. Researchers have studied VLF signal perturbations due to several possible sources of D region disturbances including solar flares (Kumar & Kumar, 2018; Raulin et al., 2013), solar eclipses (Cohen et al., 2018), geomagnetic storms (Maurya et al., 2018; Peter et al., 2006), earthquakes (Hayakawa et al., 2011; Kumar et al., 2013), and lightning associated transient luminous events (Inan et al., 1995; NaitAmor et al., 2010; Salut et al., 2012; Salut et al., 2013). However, these topics are not the part of this study.

In this work, narrowband VLF signals recorded at a low-latitude station are used to determine the D region Wait and Spies parameters for three signal paths using LWPC modeling for both daytime and nighttime conditions and comparisons are made with the previously obtained values by other researchers. Emphasis is also placed on studying the temporal variability of the D region ionospheric parameters to see how they vary over any particular night and over some days of a month. In addition, this work also tries to find out how much variability the D region can exhibit on a single night and whether the variability on a single night can be

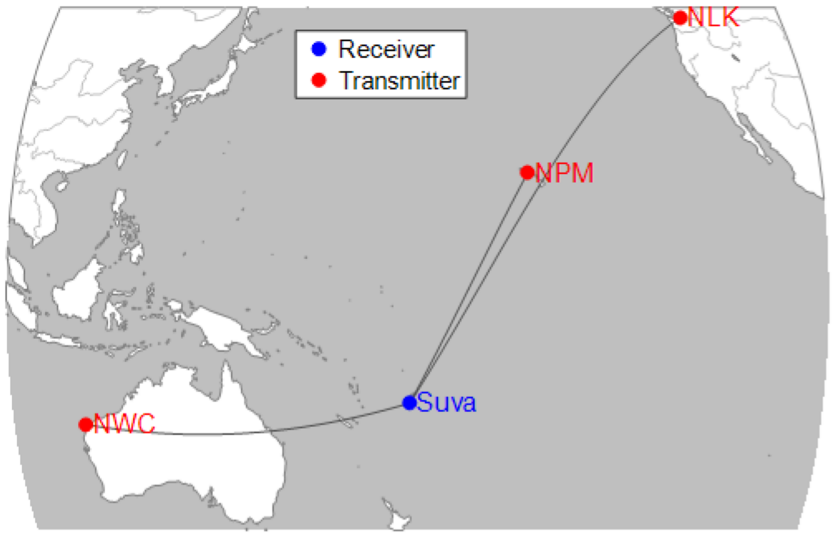

Figure 1. Map showing the transmitters and receiver (Suva, Fiji) sites and their TRGCPs.

sufficiently large as compared to the variability over several days in a month. Possible sources of nighttime signal variability and hence the nighttime *D* region ionospheric variability are discussed.

2. Data and Analysis

Investigating the ionospheric *D* region using the VLF band relies upon measurements of the amplitude and phase of subionospherically propagating coherent signals generated by VLF transmitters. A software-based VLF amplitude and phase logger, termed as "SoftPAL," was used to record the VLF signals that are minimum shift key modulated (Dowden & Adams, 2008; Kumar et al., 2008). The VLF signals were continuously logged with a resolution of 0.1 s alongside GPS-based time. Using the 0.1-s resolution data, minute-averaged values of amplitude and phase in decibels and degrees were acquired which were used to display the diurnal amplitude and phase variations. The VLF amplitude and phase data used in this work are available at the Center for Research Data repository, https://doi.org/10.4121/uuid:129f5ad8-d589-4a05-a4b7-e7cf9edfe150 (Kumar & Kumar, 2019). The TRGCPs of the NWC, NPM and NLK transmitter signals to Suva are shown in Figure 1.

To determine the daytime and nighttime ionospheric *D* region Wait and Spies parameters (H' and β), LWPC code V2.1 has been used in this work. LWPC code is an assembly of separate and self-complete programs used to model the VLF signal propagation characteristics. This code was developed by Space and Naval Warfare System center, San Diego (Ferguson, 1998), which employs an exponentially increasing conductivity with the height model of the *D* region. This simplified exponential ionospheric model is defined by two vital parameters, namely, log-linear slope (β) in the electron density and the effective VLF reference height (H') which are related by the Wait and Spies profile given by $N_e(h) = 1.43 \times 10^7[\exp(-0.15H')\exp[(\beta - 0.15)(h - H')]]$. LWPC treats the space between earth-surface and lower boundary of ionosphere as a waveguide. LWPC generates a range of amplitudes and phases as text files for various segments starting from the transmitter leading up to the receiver. In this way, the observed amplitude and phase at the receiver are obtained. Conversely, at any point, the values of H' and β can be changed using trial and error to obtain a unique pair of H' and β to match the observed amplitude and phase. Therefore, the recorded amplitude and phase of the VLF transmitter signals can provide a good measure of H' and β of the D region ionosphere.

3. Results

3.1. Morphological Features of NWC, NPM, and NLK Propagation to Suva

The NWC signal propagates mainly in west-to-east direction to the receiving station, Suva, Fiji, with a total TRGCP length of 6.69 Mm. The propagation path consists of a mixture of land and sea covering significant

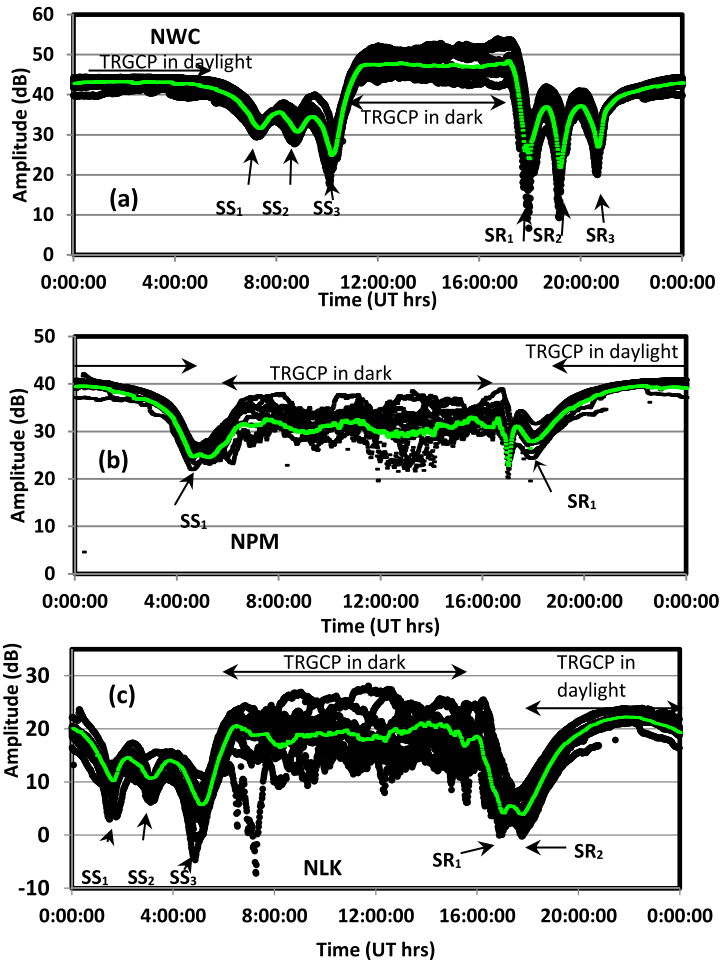

Figure 2. Diurnal variation in the amplitude of (a) NWC, (b) NPM, and (c) NLK signals for December 2009. Fifteen days of data (black plots) are over plotted to show the reproducibility of the amplitude. The average values in green are also plotted.

portion of land crossing Australia and then the ocean to Suva, as shown in Figure 1. Figure 2a shows diurnal variation in the amplitude of NWC signal for the month of December 2009. Fifteen days of amplitude data excluding the geomagnetically disturbed days chosen on the availability of continuous signals have been overplotted to indicate the reproducibility of the signal amplitude over a 24-hr period. This is achieved by first removing the VLF data of five most geomagnetically disturbed days of the month. The geomagnetic conditions data used in this paper were obtained from the WDC for Geomagnetism, Kyoto (http://wdc.kugi.kyoto-u.ac.jp/wdc/Sec3.html). The respective phase data for these months are not plotted as the phase compounds up over the days and deviates from reproducing its form. However, the uniform and stepwise phase changes correspond very well with the amplitude over the days. These curves are illustrative of those obtained at other times of the year, except for the times of occurrence of minima and their magnitude. The time used is in Universal Time (UT). The local time of Fiji is LT = UT + 12 hr. The values of signal amplitude are not calibrated since the preamplifier and antenna gains are not known. However, the values are good indicators of relative amplitude of different signals at Suva. In general, the average nighttime signal strength (~48 dB) exceeds the average daytime signal (~43 dB) giving a night-to-day signal difference and ratio of 5.0 dB and 1.78, respectively. The night-to-day signal ratio has been calculated using the average amplitude graph (green color) of Figure 2a during the midnight time of 14 hr UT (02 hr LT) and midday time of 02 hr UT (14 hr LT). The night-to-day ratio is that of the output voltage of the preamplifier at night and day obtained using the relationship $A_v\ (dB) = 20\log\frac{V_o}{1\mu V}$. NWC signal received at Suva shows three amplitude minima during both sunrise and sunset transitions labeled as SR_1, SR_2, and SR_3 and SS_1, SS_2, and SS_3,

respectively. The theory and mechanisms of signal amplitude minima formation are itself very interesting topics of study but are not subjects of consideration in this paper.

The NPM signal propagates across the geomagnetic equator over the sea largely in north-to-south direction with comparatively less in east-to-west direction (Figure 1). The total path length is about 5.07 Mm. The diurnal variation in the amplitude of NPM signal during the month of December 2009 is shown in Figure 2b. It can be seen that the signal in the nighttime of TRGCP is more variable as compared to that in the daytime but the signal reproducibility is good during both day and night propagations. In contrast to NWC, the daytime signal strength (~40 dB) is more than the nighttime signal strength (~34 dB) giving a night-to-day signal difference of −6 dB. Although the signal minima are not as distinct as in the NWC plot, a minimum each during both sunrise and sunset transitions can be identified. The amplitude minimum during sunrise is deeper and clearer than that during sunset.

The NLK signal propagates a significant path in north-to-south direction with a sufficiently large part in east-to-west direction also (Figure 1). The propagation is transequatorial and mostly over sea covering a total TRGCP length of 9.43 Mm. Figure 2c shows diurnal variation of the amplitude of NLK signal for December 2009. The day and nighttime signal strengths could be identified from the diurnal plots; daytime starting from ~18 hr UT to 02 hr UT and nighttime from 06 hr UT to 17 hr UT. It can be noted that the daytime signal strength is very stable as compared to nighttime when it is highly variable but their reproducibility can be seen. During sunset transition, three amplitude minima labeled as SS_1, SS_2, and SS_3 and during sunrise, two minima labeled as SR_1 and SR_2 are observed for the summer month of December.

3.2. *D* Region Modeling: Wait and Spies Parameters

Observed amplitude and phase of VLF signals propagating over long paths are used to determine the electron density parameters of the *D* region of the Earth's ionosphere. The paths used in this work are NWC to Suva, NPM to Suva, and NLK to Suva as shown in Figure 1. The NWC, NPM, and NLK transmitters have good amplitude stability; however, the phase records do not show good stability particularly with NLK signal. The *D* region ionospheric parameters, namely, reference height (H') in km and sharpness factor (β) in km^{-1} are modeled using the LWPC V2.1 code for the above propagation paths for December 2009 at midday and midnight for midpath of TRGCP. In addition, the variations in the nighttime signal strength for NWC and NLK are utilized to obtain the temporal variations in the H' and β and 15 days of internationally quiet geomagnetic day's amplitude data are also used to obtain the day-to-day variations in the H' and β for nighttime conditions for these two paths.

3.2.1. Daytime *D* Region Parameters

3.2.1.1. NWC-Suva Path

Daytime VLF propagation is mainly stable, resulting in clearly defined values of H' and β depicting the lower *D* region, thus allowing calculation of the received VLF amplitudes and phases (McRae & Thomson, 2000; Thomson, 1993). Like other U.S. Navy VLF transmitters, NWC typically has a very good phase and amplitude stability. However, like the other U.S. transmitters, it mostly goes off air once a week for 6–8 hr for maintenance purposes. During this period, the power radiated by the VLF transmitters goes down drastically and the recorded signal strength shows almost zero level. In the analysis, all those periods for which the signal strength falls due to power off in VLF telemetry have not been considered. Upon activation, the phase is still stable but the value of the phase (relative to GPS or UTC) is often not conserved. Additionally, in a typical week, there may be some gradual phase drift or random phase jumps (Thomson, 2010).

From the SoftPAL observed diurnal amplitudes of NWC for selected 15 days of December 2009, the mean value of the midday (00 hr UT) amplitude is found to be 42.0 dB. This mean midday amplitude will be later utilized to find the observed midnight amplitude using the day-night amplitude difference. The solar zenith angle value for mid TRGCP of the NWC-Suva path was calculated which was then used for estimation of H' and β using the relationship given by McRae and Thomson (2000). These values of H' and β were then fed into the LWPC code to obtain the midday observed values of the amplitude and phase which came as 61.1 dB and 153.2°, respectively. For long path lengths, the H' and β values can vary in between. However, in this work, we have considered the path averaged values and assume the H' and β to be uniform throughout the entire TRGCP. The LWPC codes were then run after feeding in the required information such as the TRGCP length, the bearing angle of transmitter to receiver, the receiver location and the date (10 December 2009) and midday time. The results of LWPC calculation are shown in Figure 3 for different values of H' (in the

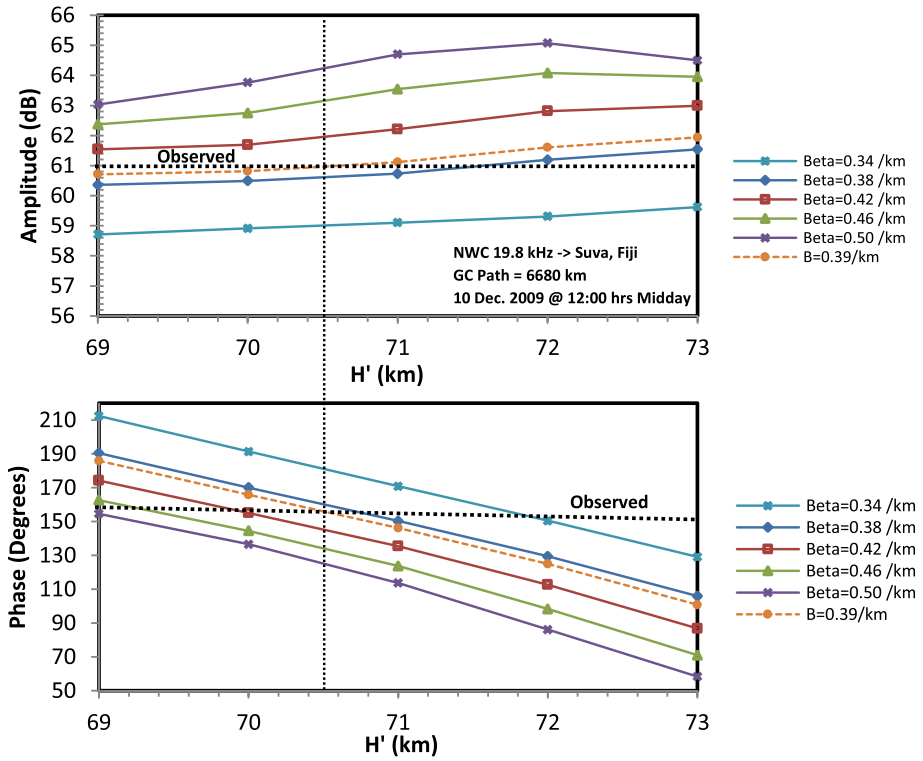

Figure 3. Comparisons of observed midday amplitude and phase (horizontal dashed lines) of NWC to Suva path with the LWPC calculated values. The dashed vertical line is used to show the estimated values of H' and β.

range 69–73 km) and β (in the range 0.34–0.50 km^{-1}), suitable for daytime propagation. The amplitudes are from LWPC's standard output in dB above 1 μV/m, assuming the radiated power of 1,000 kW. The phases are also from LWPC's standard output in degrees. The dashed horizontal lines in this figure show the daytime amplitude and phase calculated by LWPC at the receiver for the midday path for the summer date shown. From Figure 3, a unique value of H' and β needs to be determined which gives a satisfactory value for the D region. As can be seen from this Figure, a single dashed vertical line at 70.5 km crosses the observed amplitude and phase lines at the β value of 0.39 km^{-1}. The LWPC calculated graph of $\beta = 0.39$ km^{-1} is plotted to enhance the precision of estimating the H' and β parameters. Few more graphs of β close to 0.39 km^{-1} were plotted (though not shown here as the graphs become too closely spaced and indistinct) to check for a value which gives the best estimate for the H' and β using both the amplitude and phase graphs. However, the curve for β value of 0.39 km^{-1} is only plotted as it gave the best approximate. As can also be seen from the Figure 3 that the observed amplitude and phase lines can be crossing at a number of different positions hence giving various values of H' and β, therefore, the amplitude and the phase graphs together become very helpful in complementing each other so that a more accurate and unique value of the parameters can be determined. Thus, the midday D region parameters for the NWC to Suva path are estimated to be $H' = 70.5$ km and $\beta = 0.39$ km^{-1}, respectively.

3.2.1.2. NPM-Suva Path

Similar measurements were made for the NPM to Suva path with TRGCP distance of 5,095 km. The NPM has good signal reproducibility over the days and the diurnal phase could also be identified clearly though longer duration continuous phase does not show good stability and is not preserved. From the values of SoftPAL observed diurnal amplitudes for 15 days of December 2009 as shown in Figure 2b, the mean value of the midday (00 hr UT) amplitude is found to be 39.0 dB. The LWPC codes were run to obtain the midday observed values of the amplitude and phase which came as 59.05 dB and 125.1°. Again, the LWPC codes were then run after feeding in the required information such as the TRGCP length, the bearing angle of transmitter to receiver, receiver location, date (10 December 2009) and midday time. The results of LWPC calculation are shown in Figure 4 for different values of H' (in the range 69–73 km) and β (in the range 0.34–0.50 km^{-1}), relevant for daytime propagation. The dashed horizontal lines in each of these figures

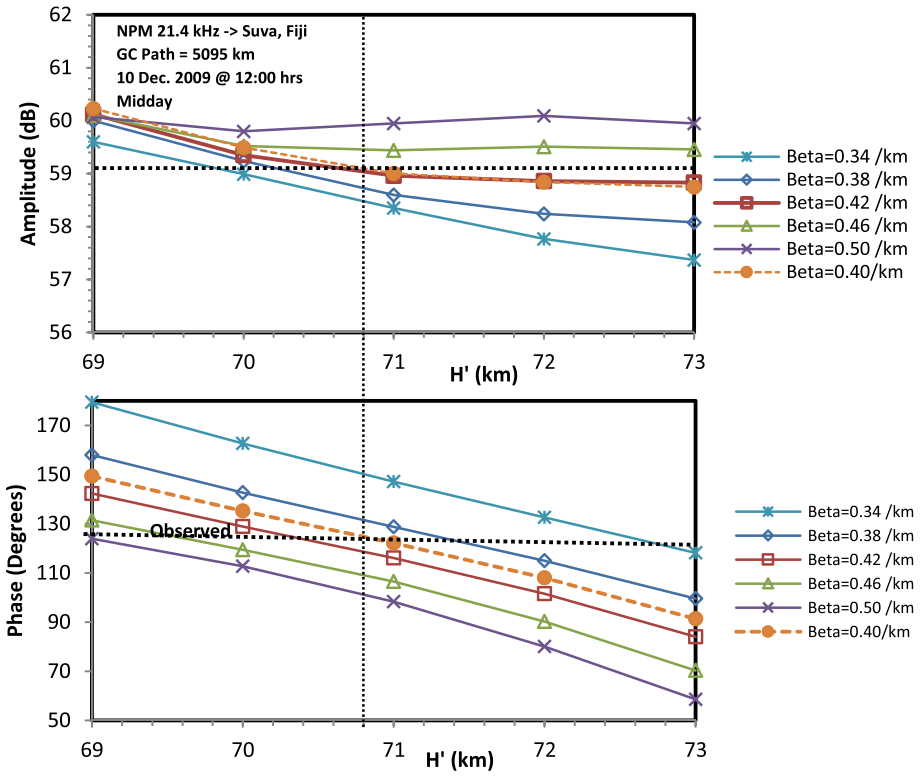

Figure 4. Comparisons of observed midday amplitude and phase (horizontal dashed lines) of NPM to Suva path with the LWPC calculated values. The dashed vertical line is used to show the estimated values of H' and β.

show the daytime amplitude and phase calculated by LWPC at the receiver for the midday path for the summer date shown. As can be seen from Figure 4, a single dashed vertical line crossing at 70.8 km crosses the observed amplitude and phase lines at the β value of 0.40 km^{-1}. The LWPC calculated graph (orange line) of $\beta = 0.40$ km^{-1} is plotted to enhance the precision of estimating the H' and β parameters. The midday D region parameters for the NPM to Suva path are estimated to be $H' = 70.8$ km and $\beta = 0.40$ km^{-1}, respectively.

3.2.1.3. NLK-Suva Path

An analysis similar to that for NWC and NPM to Suva path was carried out for NLK to Suva path with TRGCP distance of 9,220 km. From the SoftPAL observed diurnal amplitudes for 15 days of December 2009 as shown in Figure 2c, the mean value of the midday amplitude is found to be 22.0 dB. The LWPC codes were run to obtain the midday observed values of the amplitude and phase, which came as 40.2 dB and −237.5°. The results of LWPC calculation are shown in Figure 5 for different values of H' (in the range 69–73 km) and β (in the range 0.34–0.50 km^{-1}). The amplitudes are from LWPC's standard output in dB above 1 μV/m, considering the normal NLK radiated power of 192 kW and phases are also from LWPC's standard output in degrees. The dashed horizontal lines in each of these figures show the daytime amplitude and phase calculated by LWPC at the receiver for the midday path for the summer. As can be seen from Figure 5, a single dashed vertical line at 70.7 km crosses the observed amplitude and phase lines at the β value of 0.40 km^{-1}. Hence, the midday D region parameters for the NLK to Suva path are estimated to be $H' = 70.7$ km and $\beta = 0.40$ km^{-1}, respectively.

3.2.2. Nighttime *D* Region Parameters

VLF propagation at nighttime is seemingly highly variable compared to the daytime as revealed by the highly variable signal strengths (Figures 2a–2c). This is probably due to the reflecting region of the ionosphere becoming more variable and partly because the nighttime ionosphere supports greater number of modes in the EIWG which reach the receiver with substantial magnitude, thus resulting in more complex modal interference (Clilverd et al., 1999); hence, the phases and amplitudes become more sensitive to changes in the ionosphere than compared with the day. This makes it essential to take measurements

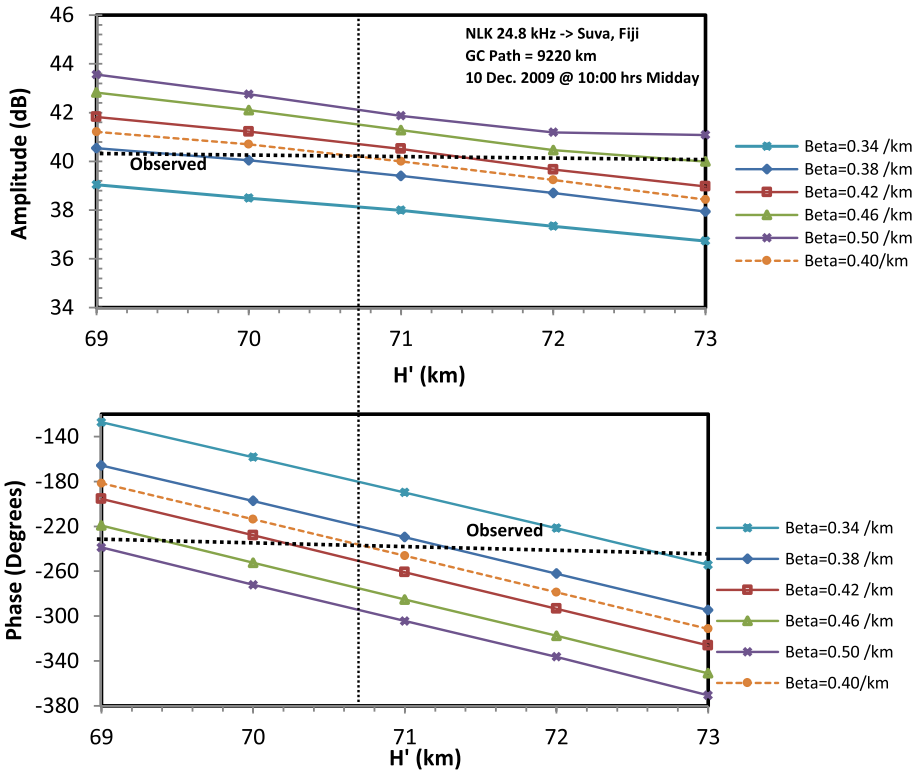

Figure 5. Comparisons of observed midday amplitude and phase (horizontal dashed lines) of NLK to Suva path with the LWPC calculated values. The dashed vertical line is used to show the estimated values of H' and β.

over several nights to institute a dependable pattern of average behavior. To determine the nighttime D region parameters, the signals from NWC, NPM, and NLK are utilized here. The modeling is carried out using the amplitude only because the LWPC V2.1 used here gives highly elevated values of phase at the nighttime in all cases, which cannot be used against the observed values to estimate the parameters. Nevertheless, approximations appear quite clear and give satisfactory values of the nighttime D region parameters.

3.2.2.1. NWC-Suva Path

From Figure 2a, the mean value of the midday amplitude of NWC is found as 42.0 dB and the midnight mean amplitude value is 48.0 dB. The difference between day and night SoftPAL recorded amplitudes (6 dB) has been added to the daytime observed amplitude of 61 dB given by LWPC to obtain the nighttime observed amplitude of 67 dB. The results of LWPC calculation are shown in Figure 6a for different values of H' (in the range 83–87 km) and β (in the range 0.50–0.80 km^{-1}), suitable for nighttime propagation on 10 December 2009. These LWPC calculated values are then combined with the observed nighttime signal amplitude as shown by the dashed horizontal line to estimate the nighttime propagation parameters. It can be seen from Figure 6a that $H' = 84.2$ km and $\beta = 0.64$ km^{-1} give a good match between observed and modeling results for NWC to Suva path.

3.2.2.2. NPM-Suva Path

The mean midday NPM amplitude is 39.0 dB obtained from Figure 3b while the midnight mean amplitude value is 34.0 dB. The difference between day and night SoftPAL recorded amplitude (~5 dB) has been subtracted from the daytime observed amplitude (for NPM, daytime signal strength is more than nighttime) determined by LWPC to obtain the nighttime observed amplitude. In this way, the nighttime observed amplitude comes out 55.0 dB. The results of LWPC calculations are shown in Figure 6b for different values of H' (in the range 83–87 km) and β (in the range 0.50–0.80 km^{-1}), relevant for nighttime propagation on 10 December 2009. These LWPC calculated values are then combined with the observed nighttime signal amplitude as shown by the dashed horizontal line to estimate the nighttime D region Wait and Spies parameters. As can be seen from Figure 6b, although the values of the ionospheric parameters are not

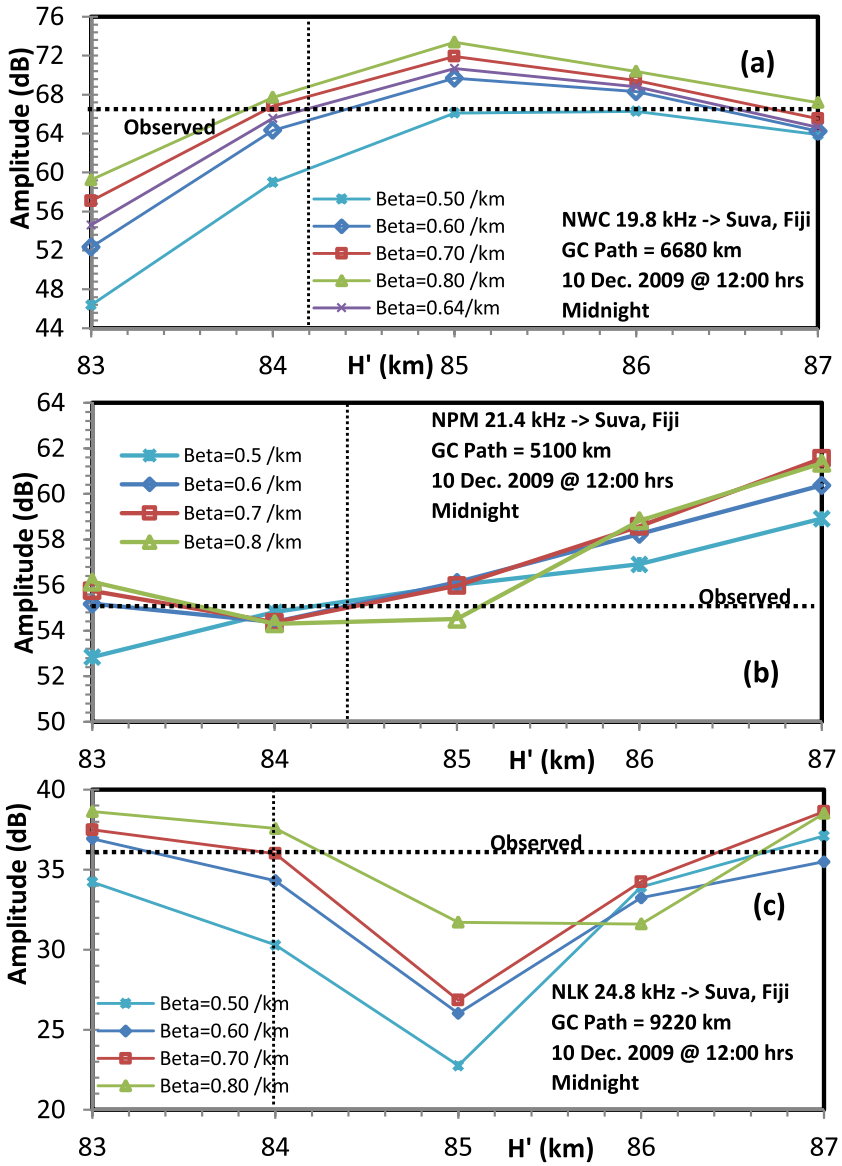

Figure 6. Comparisons of observed midnight amplitude (horizontal dashed line) of (a) NWC to Suva, (b) NPM to Suva, and (c) NLK to Suva path with the LWPC calculated values. The dashed vertical line is used to show the estimated values of H' and β.

determined definitively using LWPC and observed amplitude, the NPM to Suva results are nevertheless consistent with the nighttime ionosphere with $\beta = 0.70$ km^{-1} and $H' = 84.4$ km.

3.2.2.3. NLK-Suva Path

The SoftPAL observed diurnal amplitudes of NLK for 15 days of December 2009 overplotted in Figure 2c gives a mean midday amplitude of 22.0 dB and midnight mean amplitude of 17.4 dB. The difference between day and night SoftPAL recorded amplitude (4.6 dB) has been subtracted from the LWPC given daytime amplitude (for NLK, average daytime signal strength is more than nighttime) to obtain the nighttime observed amplitude which comes out to be 36 dB. The results of LWPC calculation are shown in Figure 6 c for H' (in the range 83–87 km) and β (in the range 0.50–0.80 km^{-1}), suitable for nighttime propagation on 10 December 2009. These LWPC calculated values are then combined with the observed nighttime signal amplitude as shown by the dashed horizontal line to estimate the nighttime H' and β parameters. Thus, it can be seen from Figure 6(c) that $H' = 84.0$ km and $\beta = 0.70$ km^{-1} give a good approximation between observed and modeling results for NLK to Suva path.

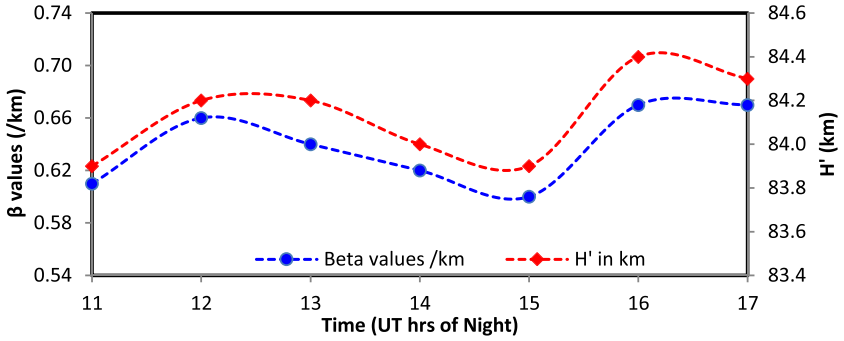

Figure 7. Temporal variation in H' and β in nighttime for NWC on 8 December 2009.

3.3. Nighttime Temporal and Day-to-Day Variability of *D* Region

3.3.1. NWC-Suva Path

The daytime VLF propagation is quite stable but VLF propagation at night is significantly variable. High temporal variability of the *D* region in the nighttime is well known but not being able to access it means that the magnitudes, time scales, and sources for variability are not well understood (Han & Cummer, 2010b).

In this section, the nighttime amplitude data of NWC and NLK signals are used to study any temporal and day-to-day variability of the nighttime H' and β parameters. The method of estimating H' and β using the LWPC calculated values and comparing with the observed values of signal amplitudes remains the same as described earlier in section 3.2. For the temporal variability at nighttime, the observed values of the amplitudes are taken at each hour and are modeled with the LWPC to estimate the temporal variation of H' and β. Similarly, the variations in the signal strength for 15 different nights at a particular hour are utilized to estimate the day-to-day variability of nighttime H' and β. To avoid any variations due to the geomagnetic activity, only geomagnetically quiet days have been considered, that is, by ignoring the five most geomagnetically disturbed days of the month.

Figure 2a shows the diurnal variation of the signal amplitude of NWC for 15 internationally geomagnetically undisturbed days for the summer month of December 2009. The signal amplitude on one of the days (08 December 2009) out of the 15 displaying the highest temporal variability has been used. The signal amplitude at each hour from 11 to 17 hr UT during which entire TRGCP was in dark has been obtained, and using the night-day amplitude difference and the method as described in section 3.2, the observed values of the nighttime amplitude is determined. Each of the observed amplitudes for each hour is then modeled using LWPC. The instantaneous values of H' and β are thus estimated for the different hours and are plotted in Figure 7. Significant variability in both the H' and β can be seen, with H' ranging between 83.9 and 84.4 km and β values ranging between 0.60 and 0.68 km^{-1} over 11–17 hr UT period of the complete nighttime of the TRGCP. In a similar manner, the H' and β parameter for a fixed hour (15 hr UT or 03 hr LT) for the 15 days has been obtained and plotted in Figure 8. Once again, a significant variability in both the H'

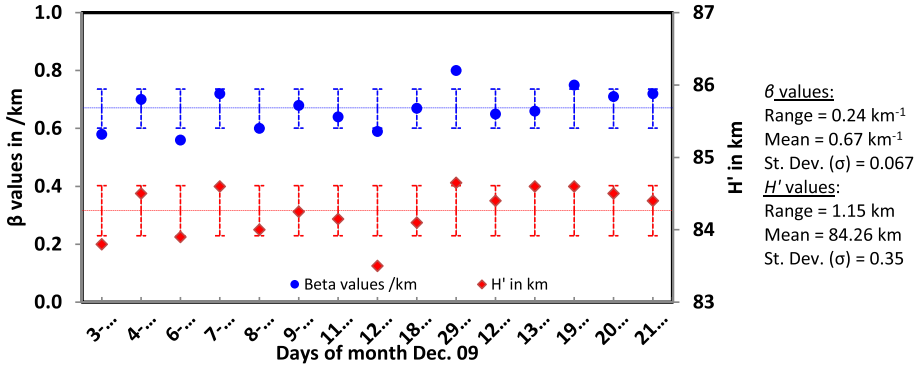

Figure 8. Variations in H' and β for NWC at 15 hr UT at night for 15 geomagnetically quiet days during December 2009. Errors bars of $\pm 1\sigma$ centered at the mean for H' and β are also plotted.

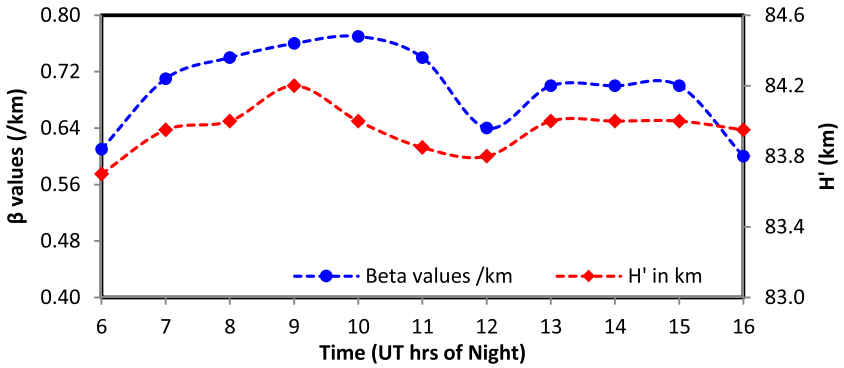

Figure 9. Temporal variation in H' and β in nighttime for NLK on 29 December 2009.

and β can be seen, with H' ranging between 83.5 and 84.7 km and β values ranging between 0.58 and 0.80 km^{-1} over the 15 days period. Hence, the statistical information derived from these values of 15 days is as follows: For β, range = 0.24 km^{-1}, mean = 0.67 km^{-1}, and standard deviation = 0.067, and for H', range = 1.15 km, mean = 84.26 km, and standard deviation = 0.35.

3.3.2. NLK-Suva Path

Figure 2c shows the diurnal variation in the amplitude of NLK for 15 geomagnetically quiet days received at Suva for the summer month of December 2009. The signal amplitude of one of the days (29 December 2009) out of the 15 displaying the highest variability has been selected. The SoftPAL signal amplitude at each nighttime hour during 06–16 hr UT has been obtained using the same procedure as that for the NWC-Suva path. The instantaneous values of H' and β, thus, estimated at the different hours are shown in Figure 9. Significant variability in both the H' and β can be seen, with H' ranging between 83.3 and 84.1 km and β values ranging between 0.50 and 0.78 km^{-1}. To study the day-to-day variability, the H' and β parameters for a fixed hour (10 hr UT or 22 LT), for the 15 undisturbed days have been obtained and plotted in Figure 10. Once again, a significant variability in both the H' and β can be seen in Figure 10, with H' ranging between 83.0 and 85.2 km and β values ranging between 0.58 and 0.82 km^{-1} over the 15-day period. The statistical information derived from these values of 15 days for NLK is as follows: For β, range = 0.24 km^{-1}, mean = 0.71 km^{-1}, and standard deviation = 0.081, and for H', range = 2.2 km, mean = 83.72 km, and standard deviation = 0.79.

4. Discussion

The D region ionosphere is mainly ionized by Lyman-α and other radiations such as X-rays, galactic cosmic rays, and EUV radiation. According to Strobel et al. (1974), scattered Lyman-α is an important source of nighttime D region ionization at the low and midlatitudes. The geocoronal Lyman-α and Lyman β which photoionize NO and O_2, respectively, are other sources of nighttime D region ionization at the low latitudes

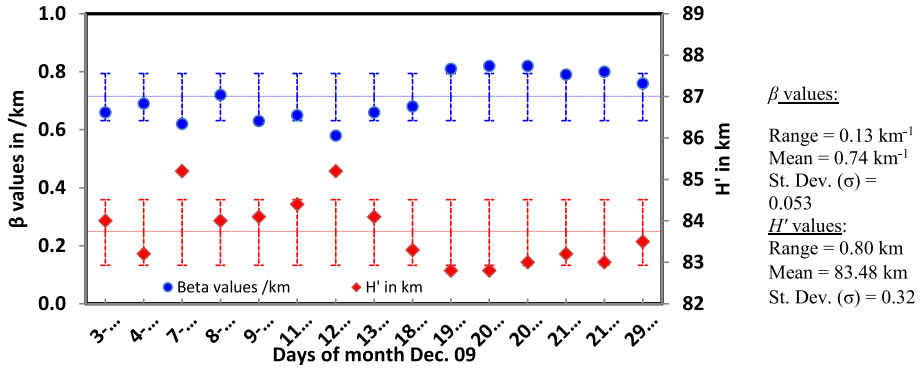

Figure 10. Variations in H' and β for NLK at 10 hr UT at night for 15 geomagnetically undisturbed days during December 2009. Errors bars of $\pm 1\sigma$ centered at the mean for H' and β are also plotted.

Table 1
Average Signal Strengths of the VLF Signals Received at Suva

Received signal at Suva	Average signal strengths (dB)		Night-day signal difference (dB)
	complete nighttime	complete daytime	
NWC	48	43	5
NPM	34	40	−6
NLK	20	23	−3

(Banks & Kockarts, 1973; Thomson et al., 2007). In the *D* region, the increasing atmospheric density absorbs the solar radiation and the electron attachment and recombination rates become so high that the free electron density becomes very small.

4.1. Morphological Features of Subionospheric VLF Propagation

The amplitude and phase study of three VLF signals propagating over long paths (>5 Mm) presented in this work shows a number of diurnal features, of which, the distinct difference between day and night signal strength and the formation of sunrise and sunset minima are of prominence. VLF signals propagate as in waveguide modes through the EIWG. The intensity of each mode depends on a number of factors including TRGCP distance, path attenuation, surface conductivity, transmitter power, ionospheric height, the excitation of modes, and direction of propagation (Snyder & Pappert, 1969; Wait, 1957). In general, as the distance between the receiver and the transmitter increases, the signal strength decreases due to an increase in attenuation with distance. The signals during nighttime suffer less attenuation compared to the daytime due to enhanced conductivity of the ionosphere where VLF signals undergo mirror-like reflection compared to diffusive type from the *D* region in the daytime (Crombie et al., 1958). The signals considered in this study would have different attenuations because they travel different path lengths with mixture land and sea-based paths.

Based on the results, under pure daytime propagation, the average signal strengths are as follows: NWC = 43 dB, NPM = 40 dB, and NLK = 23 dB as listed in Table 1. Under pure nighttime propagation the signal strengths are as follows: NWC = 48 dB, NPM = 34 dB, and NLK = 20 dB. Since transmitter power and propagation distance for all transmitters are different, it is worth examining the difference in the observed night and day signal strengths. The difference between the night and day signal strengths for these three signals are as follows: NWC = 5 dB, NPM = -6 dB, and NLK = -3 dB (negative values indicate that the daytime signal strengths are more than the nighttime). One of the reasons for negative night-day difference in amplitude over long paths where the daytime amplitude is more than nighttime such as for NPM and NLK contrary to NWC could be because of daytime position of the receiving station being near the constructive interference for NPM and NLK signals resulting in larger daytime amplitude as compared to nighttime (Figure 11). NWC signal mainly propagates from west to east whereas NPM and NLK signals have east-west propagation component. Crombie et al. (1958) reported that VLF signals traveling from west are less attenuated than the signals traveling from east, but this will not affect the day and nighttime signal strength differences and neither the Wait and Spies parameters. However, NPM and NLK signals are propagating from east; hence, they may be incurring more attenuation compared to the NWC signal.

The LWPC modeled output for signal strength versus distance from NWC, NPM, and NLK signals during daytime and nighttime is presented in Figure 11. The vertical lines in the panels indicate the position of the receiver away from the transmitter. The horizontal guidelines indicate the signal strength and the modal position at the receiver. The modal plots depict that the nighttime signal strengths (NPM = 57 dB and NLK = 26 dB) are less when compared to the daytime signal strengths (NPM = 58 dB and NLK = 30 dB) for the NPM and NLK signals, hence the observed difference. Contrary to this for the NWC signal, the modal graphs indicate that the nighttime signal strength is more (63 dB) when compared to the daytime signal strength (55 dB), which is well reflected from the observed values as well. LWPC modeling showed the existence of eight daytime modes for these transmitter paths to Suva whereas for nighttime propagation it showed 11, 18, and 16 modes for NWC, NPM, and NLK paths, respectively. The higher order modes suffer more attenuation than the lower order modes, for example, during the daytime, the attenuation of lower order modes (modes 1 and 2) is 2–4 dB/Mm while higher order modes (mode 8) have attenuation of up to 40 dB/Mm. Generally, the nighttime signal strength at any site can be higher or lower than the daytime signal strength. There can be many modes propagating during both day and nighttime. The complex interference between different modes results in series of minima and maxima in the VLF signals propagating between the transmitter and the receiver as shown in the modal graphs of Figure 11. Carefully looking at the LWPC generated graphs of Figure 11, at any fixed location between the transmitter and receiver, the signal strength may be more in the nighttime than daytime and vice versa. It entirely depends where the receiving station is located along

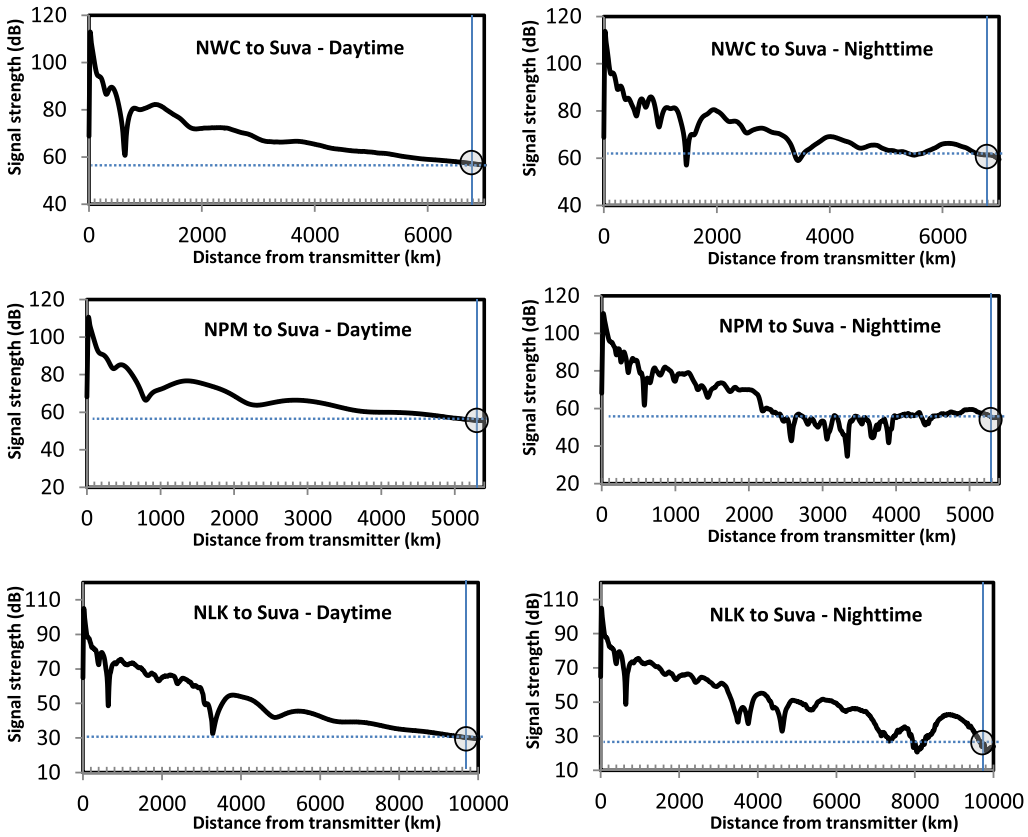

Figure 11. LWPC output for signal strength versus distance from the transmitter for NWC, NPM, and NLK signals during daytime and nighttime. The vertical lines in the panel indicate the position of the receiver away from the transmitter. The horizontal guide lines indicate the signal strength and the modal position at the receiver.

the modal distribution; it can be at a null position at nighttime, thereby exhibiting a low signal value as compared to the daytime.

Dowden et al. (1996) stated that attenuation of the second-order mode in the daytime is very high, approximately 10 dB higher than the first-order mode over the daytime path. Clilverd et al. (1999) using LWPC code modeled the nighttime propagation of NAA to the Faraday (Antarctica) path. Their results depicted gradual decrease in amplitude with distance. There were positions where amplitude was significantly reduced (minima) and enhanced (maxima) due to interference between the propagating modes. Similar results of amplitude (sum of all modes) versus distance from NAA transmitter for four different ionospheric profiles were obtained by Bainbridge and Inan (2003). Due to higher attenuation of modes in the daytime compared to nighttime and the position of Suva for NWC-Suva path lying around the modal maximum in the nighttime and minimum in the daytime, the observed signal strength in the nighttime is more than in the daytime. However, for NPM-Suva and NLK-Suva path, the position of Suva appears to be around a modal minimum in the nighttime and a modal maximum in the daytime, giving greater signal strength in the daytime as compared to the nighttime. Johnson (2000) suggested that multiple modes could exist between transmitter and receiver, which can interfere destructively, yielding the nighttime amplitude lower than the day at certain positions along the TRGCP. Since the path length of NPM-Suva TRGCP is 5,070 km over sea, there is a possibility that multiple modes may exist in the nighttime and daytime propagation paths as well producing complex interference pattern (for example, LWPC output indicates 16 modes for NPM signal at nighttime when compared to 11 modes for NWC). The multiple modes at nighttime for NPM signal may interfere destructively giving lower signal strength when compared to the daytime signal.

4.2. D region Modeling

The amplitude and phase data from VLF transmitter signals (NWC, NPM, and NLK) for long paths to Suva are utilized to estimate the daytime and nighttime D region parameters, H', and β, and are summarized in

Table 2
D Region Parameters Obtained From LWPC Modeling

VLF signal paths	Daytime		Nighttime	
	H' (km)	B (km^{-1})	H' (km)	B (km^{-1})
NWC-Suva	70.5	0.39	84.2	0.64
NPM-Suva	70.8	0.40	84.4	0.70
NLK-Suva	70.7	0.40	84.0	0.70

Table 2. The results obtained are compared with the previously obtained values of H' and β by (Thomson et al., 2007; Thomson & McRae, 2009; Thomson, 2010; Thomson et al., 2011) for paths of similar lengths and propagations. Generally, a good agreement is found between them. Though the modeling results by LWPC V2.1 seems better, it may not be perfect as there is a degree of trial and error involved in estimation of the parameters and there could be some differences in the values obtained from those reported by Thomson et al. [2007–2011] who used the earlier model of LWPC V2.0 which did not incorporate the more recent values of standard parameters such as magnetic field variations along the paths.

For NWC to Suva path, the daytime values of $H' = 70.5$ km and $\beta = 0.39$ km^{-1} are close to those obtained by Thomson (2010) for the short path from NWC to Karratha/Dampier of $H' = 70.5$ km and $\beta = 0.47$ km^{-1}. The differences in β could be because of the path length difference in the two propagations, where NWC to Suva path is 6,680 km and NWC to Karratha is just ~300 km (a relatively shorter path). The nighttime values of $H' = 84.2$ km and $\beta = 0.64$ km^{-1} are also quite similar to the values obtained for NWC to Madagascar path (long, low latitude nonequatorial path similar to NWC-Suva) of $H' = 84$-85 km and $\beta = 0.6$-0.8 km^{-1}.

For NPM to Suva path, the daytime values of $H' = 70.8$ km and $\beta = 0.40$ k^{-1} are similar to those obtained by Thomson et al. (2011) for the long path from NPM to Dunedin of $H' = 70.8$ km and $\beta = 0.46$ km^{-1}. The differences in β could again be due to the path length difference in the two propagations, where NPM to Suva path is 5,100 km and NPM to Dunedin is 8,122 km (a relatively longer path). Also, the NPM to Dunedin path covers good distance in the low to mid latitude range whereas NPM to Suva path is in the low latitude region. The nighttime values of $\beta = 0.70$ km^{-1} and $H' = 84.4$ km are also quite similar to the values obtained for NPM to Dunedin (long, transequatorial path similar to NPM-Suva) of $H' = 85$ km and $\beta = 0.65$ km^{-1}. Once again, the small differences in the H' and β could be due to the path length difference between the two paths, error in estimating the H' and β, and different versions of LWPC used.

For a very long NLK to Suva path, the daytime values of the D region parameters obtained are $H' = 70.7$ km and $\beta = 0.40$ km^{-1}. Similar values of $H' = 70.9$ km and $\beta = 0.435$ km^{-1} were obtained by Thomson et al. (2011) for a very long NLK to Dunedin path. The nighttime values of $H' = 84.0$ km and $\beta = 0.70$ km^{-1} are also quite similar to the values obtained for Omega Japan to Dunedin (long, transequatorial path similar to NLK-Suva) in the range of $H' = 83$–87 km and $\beta = 0.50$–0.70 km^{-1}. The exact values of the parameters were not reported as the estimates were not very clear for the above path as reported by Thomson and McRae (2009).

Generally, it is seen here that the estimated H' values are in very good agreement with what Thomson et al. (2007–2011) have reported for similar paths as considered here. However, some differences in the β values can be seen from the ones obtained in this study to those reported previously. One of the reasons for the differences could be because of the different version of LWPC (V2.1) used here when compared with the old version (V2.0) used in the previous studies. A test was made with LWPC V2.1 for paths used by Thomson and McRae (2009) who used V2.0, and slight differences in the calculated values of the amplitudes and phases were seen which could have contributed to slight differences in the obtained values of H' and β. The differences in the values of β obtained here could also be due to the differences in the distance covered by the TRGCPs for different latitude range. Thomson et al. (2011) have shown a relationship between the β variations with the geomagnetic latitude for near overhead sun (in summer) near solar minimum. They found that the β value changes as the TRGCP traverses more toward the higher latitudes and obtained the relationship between the β and the geomagnetic latitude (λ) described by the equation, $\beta(\lambda) = 0.47 - (0.47 - 0.34)\,(Q_\lambda - Q_{30})/(Q_{53.5} - Q_{30})$, where Q is the ion-pair production rates at different latitudes (λ).

For near midday, Thomson (1993) found $H' = 70.0$ km and $\beta = 0.45$ km^{-1} during solar maximum while NOSC found $H' = 70.0$ km and $\beta = 0.50$ km^{-1} for summer (path descriptions given in section 1.0). The current results presented here for 2009 (average values for three paths are $H' = 70.7$ km and $\beta = 0.40$ km^{-1}), however, are for solar minimum for which McRae and Thomson (2000) found similar values of $H' = 70.7$ km and $\beta = 0.39$ km^{-1}. This low value of β obtained during solar minimum could be due to the enhanced galactic cosmic rays thereby increasing the electron density in the midlatitude in the lower region of the

VLF reflection height range compared to the slightly reduced Lyman-α ionization in the upper part of this height range (Thomson & Clilverd, 2001). The galactic cosmic rays are omnidirectional, and their strength in the *D* region does not fluctuate with time of day; however, intensity varies significantly with geomagnetic latitude, being evidently higher in Polar Regions than near the equatorial regions (Thomson et al., 2014).

Thomson et al. (2007) using a large set of VLF amplitude and phase observations and LWPC modeling found that the nighttime averaged H' and β over many days, for the midlatitude *D* region near solar minimum to be 85.1 $\pm$ 0.4 km and 0.63 $\pm$ 0.04 km^{-1}, respectively. From the results presented here for the three long low latitude/low-midlatitude paths (one nonequatorial and two transequatorial), the average values of the nighttime *D* region parameters estimated are $H' = 84.2$ km and $\beta = 0.68$ km^{-1}. Once again, some differences in the values obtained in this work are seen from those reported by Thomson et al. (2007) and can be attributed to the reasons as already mentioned. In addition, the approximations using the LWPC calculations and the observed values of the amplitudes only for the nighttime could be limiting the accuracy with which these parameters have been estimated. LWPC V2.1 used here gives highly elevated values of phase at the nighttime in all cases, which cannot be used against the observed values to estimate the parameters. The estimated values of β for the NPM and NLK paths (~0.70 km^{-1}) seem to be slightly higher. Both these paths are transequatorial and according to Thomson and McRae (2009); the effects of irregularities in the equatorial electrojet may extend down into the nighttime D region (Gossard, 1970; Jianqi Qin et al., 2014) which can account for the observed VLF perturbations through scattering or mode conversion. These irregularities due to trans-equatorial path observations are found to be often not well modeled by LWPC.

4.3. Nighttime Variability of the *D* Region

The obvious feature seen from the diurnal plots is the high variability of the nighttime signal strength compared to the daytime. Ries (1967) proposed that the mode conversion factor at the day-night terminator and the second mode attenuation in the sunlit part of the propagation path must be sufficiently high. Considering multiple modes in the night and at least two modes in the day, Clilverd et al. (1999) suggested that the low variability of the daytime signal is due to the presence of fewer modes to interfere. In the night, the variability becomes high because of the increase in the number of significant modes (five or more) and the consequent interference between them. This is found to be true for both NWC and NLK as their amplitudes in the daytime have very small variability when compared to the nighttime amplitudes. The day-to-day and temporal variability of the nighttime ionosphere also seems to be the contributing factor for the high nighttime variability of signals (Han & Cummer, 2010a, b).

For both the NWC and NLK signal paths analyzed for the nighttime variability, the variations in H' (range ~2.0 km) and β (range ~0.2 km^{-1}) are found to be substantial. This implies that the nighttime VLF signal variability is caused by the variation in the *D* region reflection height and the electron density gradient changes. This results in changes in attenuation, which is why the signals amplitude varies a lot at nighttime. The magnitude of the hourly H' and β variation (range H' ~0.5 km, β ~0.15 km^{-1}) on a single night is almost as large as the observed day-to-day variation (range H' ~1.0 km, β ~0.2 km^{-1}) for 15 quiet nights across the entire month period. This indicates that much of the nighttime *D* region dynamics can occur on time scales less than a day. It can also be interpreted from Figures 8 and 10 that H' and β values can deviate by more than one standard deviation from the mean nighttime values on any night of the month. NLK signal has considerably larger variability as compared to NWC, probably due to its longer propagation path and the larger range of local time zones traveled.

Han and Cummer (2010b) studied the *D* region ionospheric parameters (H' and β) by measuring the high-power broadband VLF signals generated by the lightning flashes. They broadband sferic data was analyzed by these authors recorded during July and August 2005 by the instruments located near Duke University, USA. They extracted the height of an assumed exponential electron density profile for each measurement by comparing measured sferic spectra to the finite difference time domain (FDTD) simulation results. The *D* region electron density profile showed large temporal variations of many kilometers on some nights and relatively unchanging behaviors on others. The temporal variability on some nights displayed a close correlation with the occurrence rate of lightning discharges in the region of study. This implied that the direct energy coupling between lightning discharges and lower ionosphere could be a significant source of variability in the nighttime *D* region. However, the measured height temporal variability on some nights exhibited weak or almost no correlation with local lightning or geomagnetic activities. Their

measurements suggested that many other processes might drive nighttime *D* region variability. They estimated hourly H' between 82.0 and 87.2 km with a mean value of 84.9 km and standard deviation of 1.1 km.

Maurya et al. (2012) used the tweek sferics observed during 2010 simultaneously at two low-latitude Indian stations, Allahabad and Nainital, to estimate the day-to-day variability in H' and β and obtained about 5 km and 0.2 km^{-1}, respectively, which at any hour varied in the range of 4 km and 0.18 km^{-1}.

Scattered Lyman-α is the main source of mid and low latitude *D* region ionization at nighttime (Banks & Kockarts, 1973; Strobel et al., 1974). High-energy radiation belt electron precipitation also contributes to ionization but at mid to high latitudes. The causes of this precipitation can be the interaction between energetic particles and whistler waves (Blake et al., 2001; Jasna et al., 1992; Rodger et al., 2003). However, this is very unlikely for the low-latitude NWC-Suva path as the entire TRGCP has low magnetic L-shell values ($L < 1.5$) where whistler-induced electron precipitations have hardly been observed (Voss et al., 1998). However, NLK signal with portion of its TRGCP located at $L > 1.5$ propagates from middle to high latitude where whistler-induced electron precipitations can occur (Voss et al., 1998); hence, NLK signal may register classic VLF events also giving rise to high temporal and day-to-day *D* region variability. Direct coupling of lightning-ionosphere can also affect *D* and *E* region ionosphere variabilities. Electromagnetic pulses radiated by lightning can directly link into the lower ionosphere, heating the electrons, thereby changing the ionization rate and perturb the VLF signal propagation (Inan et al., 1993), which is more noticeable at low latitudes. The geomagnetic activity could also be linked to the increase in *D* region variability; however, little/no connection can be made between this and the measured H' and β as the days studied here were only from internationally recognized quiet geomagnetic days. The gravity waves of Meteorological origin (*e.g.,* tropical cyclones, mesoscale convective systems, tornados, and upper troposphere jet) (Laštovička, 2009; NaitAmor et al., 2018), coming to ionosphere from below could also contribute to the day-to-day variability of the nighttime D region which is an area of further research. The D region plasma irregularities associated with strong thunderstorm and meteor events could also contribute to the short time scale D region variability (Gossard, 1970; Jianqi Qin et al., 2014).

5. Summary and Conclusions

The VLF signals from the three navigational transmitters, NWC, NPM, and NLK, are utilized to study their morphological features of propagation. The observed amplitude and phase of these signals have been used to determine the daytime and nighttime *D* region ionospheric parameters (H' and β) for the different propagation paths using LWPC modeling. The daytime *D* region of the ionosphere is pretty stable and predictable giving well-defined values of H' and β, but at nighttime, the signal variability is very high. As such, the temporal variability of the nighttime *D* region ionosphere is also studied to see how the ionospheric parameters change during different hours of the night as well as how they vary at any particular hour over the days. The main conclusions drawn from this work are as follows:

- Under pure daytime propagation, the average signal strength as recorded by SoftPAL is; NWC = 43.0 dB, NPM = 40.0 dB, and NLK = 23.0 dB and under pure nighttime propagation the strength is NWC = 48.0 dB, NPM = 34.0 dB, and NLK = 20.0 dB. The difference between the night and day signal strength is NWC = 5.0 dB, NPM = - 6.0 dB, and NLK = −3.0 dB. The negative value indicates that the daytime signal strength is more than nighttime. This difference in the signal strength can be attributed to the different attenuation rates of the signals over the day and nighttime paths together with the difference in the modal position of the receiver from the transmitter.
- The daytime *D* region parameters for the three propagation paths estimated using LWPC modeling are as follows; for NWC, $H' = 70.5$ km and $\beta = 0.39$ km^{-1}, for NPM, $H' = 70.8$ km and $\beta = 0.40$ km^{-1}, and for NLK, $H' = 70.7$ km and $\beta = 0.40$ km^{-1}. The nighttime *D* region parameters for the three paths estimated are as follows: for NWC, $H' = 84.2$ km and $\beta = 0.64$ km^{-1}, for NPM, $H' = 84.4$ km and $\beta = 0.70$ km^{-1}, and for NLK, $H' = 84.0$ km and $\beta = 0.70$ km^{-1}.
- An appreciable nighttime temporal and day-to-day *D* region variability is found, where H' varied between 83.5 and 84.7 km for NWC and 83.0 and 85.2 km for NLK, while β typically varied between 0.58 and 0.80 km^{-1} for NWC and 0.58 and 0.82 km^{-1} for NLK signals. The nighttime signal variability could be accounted to complex interference pattern arising from the presence of larger number of significant modes and *D* region perturbations due to strong flashes of lightning, planetary waves, tides, and

traveling ionospheric disturbances associated gravity waves due to various sources including natural hazards such as tropical cyclones and earthquakes.

Acknowledgments
The authors thank the Research Committee of the Faculty of Science, Technology, and Environment, The University of the South Pacific (USP), for their initial financial support to carry out this work. The authors are also thankful for financial support by USP's main research office under the funding name Strategic Research Theme (2017), grant funding number F7304-RI001-ACC-001) under which a part of work has been carried out. Authors are also thankful to S. A. Cummer, Electrical and Computer Engineering Department, Duke University, USA, for his useful suggestions on the draft manuscript. The VLF data is available at the Centre for Research Data repository and can be obtained from https://doi.org/10.4121/uuid:129f5ad8-d589-4a05-a4b7-e7cf9edfe150 website.

References

Bainbridge, G., and U. S. Inan (2003), Ionospheric D region electron density profiles derived from the measured interference pattern of VLF waveguide modes, *Radio Science 38*(4): doi: https://doi.org/10.1029/2002RS002686. ISNN: 0048-6604.

Banks, P. M., & Kockarts, G. (1973). *Aeronomy*. New York: Academic.

Blake, J. B., Inan, U. S., Walt, M., Bell, T. F., Bortnik, J., Chenette, D. L., & Christian, H. J. (2001). Lightning-induced energetic electron flux enhancements in the drift loss cone. *Journal of Geophysical Research*, *106*(A12), 29,733–29,744.

Cheng, Z., Cummer, S. A., Baker, D. N., & Kanekal, S. G. (2006). Nighttime D region electron density profiles and variabilities inferred from broadband measurements using VLF radio emissions from lightning. *Journal of Geophysical Research*, *111*, A05302. https://doi.org/10.1029/2005JA011308

Clilverd, M. A., Thomson, N. R., & Rodger, C. J. (1999). Sunrise effects on signals propagating over a long north-south path. *Radio Science*, *34*, 939–948.

Cohen, M. B., Gross, N. C., Higginson-Rollins, M. A., Marshall, R. A., Gołkowski, M., Liles, W., et al. (2018). The lower ionospheric VLF/LF response to the 2017 great American solar eclipse observed across the continent. *Geophysical Research Letters*, *45*. https://doi.org/10.1002/2018GL077351

Comité Consultatif International des Radiocommunications: Düsseldorf, Questions du CCIR (1990). Commissions d'Études 11. *15*.

Crombie, D. D. (1964). Periodic fading of VLF signals received over long paths during sunrise and sunset. *Journal of Research National Bureau of Standards, Radio Science D*, *68B*(1), 27–35.

Crombie, D. D., Allan, A. H., & Newman, M. (1958). Phase variation of 16 kc/s transmissions from Rugby as received in New Zealand. *Proceedings of the Institute of Radio Engineers*, *105*, 301–304.

Cummer, S. A., Inan, U. S., & Bell, T. F. (1998). Ionospheric D region remote sensing using VLF radio atmospherics. *Radio Science*, *33*, 1781–1792.

Dowden, R. L., and C. D. D. Adams (2008) SoftPAL, Proceedings of the 3rd VERSIM Workshop, Tihany, Hungary, 15-20 September.

Dowden, R. L., Brundell, J. B., Lyons, W. A., & Nelson, T. E. (1996). Detection and location of red sprites by VLF scattering of subionospheric transmissions. *Geophysical Research Letters*, *23*, 1737–1740.

Ferguson, J. A. (1998), Computer Programs for assessment of Long-Wavelength Radio Communications, Version 2.0., Technical document 3030, Space and Naval Warfare Systems Center, San Diego.

Ferguson, J. A., and F. P. Snyder (1990), Computer programs for assessment of long wavelength radio communications, version 1.0: Full FORTRAN code user's guide, Naval Ocean Syst. Cent. Tech. Doc. 1773, DTIC AD-B144 839, Defense Tech. Inf. Cent., Alexandria, Va.

Gossard, E. E. (1970). Irregularities in ionization of the nighttime D region deduced from vertically incident VLF radio waves. *Radio Science*, *5*, 7–17.

Han, F., & Cummer, S. A. (2010a). Midlatitude daytime D region ionosphere variations measured from radio atmospherics. *Journal of Geophysical Research*, *115*, A10314. https://doi.org/10.1029/2010JA015715

Han, F., & Cummer, S. A. (2010b). Midlatitude nighttime D region ionosphere variability on hourly to monthly time scales. *Journal of Geophysical Research*, *115*, A09323. https://doi.org/10.1029/2010JA015437

Han, F., Cummer, S. A., Li, J., & Lu, G. (2011). Daytime ionospheric D region sharpness derived from VLF radio atmospherics. *Journal of Geophysical Research*, *116*, A05314. https://doi.org/10.1029/2010JA016299

Hayakawa, M., Raulin, J. P., Kasahara, Y., Bertoni, F. C. P., Hobara, Y., & Guevara-Day, W. (2011). Ionospheric perturbations in possible association with the 2010 Haiti earthquake, as based on medium-distance subionospheric VLF propagation data. *Natural Hazards and Earth System Sciences*, *11*, 513–518.

Inan, U. S., Bell, T. F., Pasko, V. P., Sentman, D. D., Wescott, E. M., & Lyons, W. A. (1995). VLF signatures of ionospheric disturbance associated with sprites. *Geophysical Research Letters*, *22*, 3461–3464.

Inan, U. S., Rodriguez, J. V., & Idone, V. P. (1993). VLF signatures of lightning-induced heating and ionization of the nighttime D region. *Geophysical Research Letters*, *20*(21), 2355–2358.

Jasna, D., Inan, U. S., & Bell, T. F. (1992). Precipitation of suprathermal (100 EV) electrons by oblique whistler waves. *Geophysical Research Letters*, *19*(16), 1639–1642. https://doi.org/10.1029/92GL01811

Jianqi Qin, J., Pasko, V. P., McHarg, M. G., & Stenbaek-Nielsen, H. C. (2014). Plasma irregularities in the D region ionosphere in association with sprite streamer initiation. *Nature Communications*, *5*, 3740. https://doi.org/10.1038/ncomms4740

Johnson, M. P. (2000), VLF Imaging of lightning-induced ionospheric disturbances, Ph.D. Thesis, Department of Electrical Engineering, Stanford University.

Kumar, A., & Kumar, S. (2018). Solar flare effects on D-region ionosphere using VLF measurements during low- and high-solar activity phases of solar cycle 24. *Earth, Planets and Space*, *70*, 29. https://doi.org/10.1186/s40623-018-0794-8

Kumar, A., and S. Kumar (2019), Very low frequency (VLF) data obtained from Navigational Transmitters used to model the D region ionosphere. 4TU.Centre for Research Data. Dataset. https://doi.org/10.4121/uuid:129f5ad8-d589-4a05-a4b7-e7cf9edfe150.

Kumar, A., Kumar, S., Hayakawa, M., & Menk, F. (2013). Subionospheric VLF perturbations observed at low latitude associated with earthquake from Indonesia region. *Journal of Atmospheric and Terrestrial Physics*, *102*, 71–80. https://doi.org/10.1016/j.jastp.2013.04.011

Kumar, S., Kumar, A., & Rodger, C. J. (2008). Subionospheric early VLF perturbations observed at Suva: VLF detection of red sprites in the day. *Journal of Geophysical Research*, *113*, A03311. https://doi.org/10.1029/2007JA012734

Laštovička (2009). Forcing of the ionosphere by waves from below. *Journal of Atmospheric and Terrestrial Physics*, *68*, 479–497.

Maurya, A. K., Veenadhari, B., Singh, R., Kumar, S., Cohen, M. B., Selvakumaran, R., et al. (2012). Nighttime D region electron density measurements from ELF-VLF tweek radio atmospherics recorded at low latitudes. *Journal of Geophysical Research*, *117*, A11308. https://doi.org/10.1029/2012JA017876

Maurya, A. K., Venkatesham, K., Kumar, S., Singh, R., Tiwari, P., & Singh, A. K. (2018). Effects of St. Patrick's Day geomagnetic storm of March 2015 and of June 2015 on low-equatorial D region ionosphere. *Journal of Geophysical Research, Space Physics*, *123*, 6836–6850. https://doi.org/10.1029/2018JA025536

McRae, W. M., & Thomson, N. R. (2000). VLF phase and amplitude: Daytime ionospheric parameters. *Journal of Atmospheric and Solar - Terrestrial Physics*, *62*(7), 09–618. https://doi.org/10.1016/S1364-6826(00)00027-4

Morfitt, D. G. (1977), Effective electron density distributions describing VLF/LF propagation data, NOSC TR *141*.

Morfitt, D. G., and C. H. Shellman (1976) MODESRCH, an improved computer program for obtaining ELF/VLF/LF propagation data, Naval Ocean Systems Center Tech. Report. NOSC/TR 141, NTIS Accession No. ADA047508, National Technical Information Service, Springfield, VA 22161, U.S.A.

Naitamor, S., Alabdoadaim, M. A., Cohen, M. B., Cotts, B. R. T., Soula, S., Chanrion, O., et al. (2010). VLF observations of ionospheric disturbances in association with TLEs from the Eurosprite 2007 campaign. *Journal of Geophysical Research*, *115*, A00E47. https://doi.org/10.1029/2009JA015026

NaitAmor, S., Cohen, M. B., Kumar, S., Chanrion, O., & Neubert, T. (2018). VLF signal anomalies during cyclone activity in the Atlantic Ocean. *Geophysical Research Letters*, *45*. https://doi.org/10.1029/2018GL078988

Peter, W. B., Chevalier, M. W., & Inan, U. S. (2006). Perturbations of midlatitude subionospheric VLF signals associated with lower ionospheric disturbances during major geomagnetic storms. *Journal of Geophysical Research*, *111*, A03301. https://doi.org/10.1029/2005JA011346

Raulin, J.-P., Trottet, G., Kretzschmar, M., Macotela, E. L., Pacini, A., Bertoni, F. C. P., & Dammasch, I. E. (2013). Response of the low ionosphere to X-ray and Lyman-α solar flare emissions. *Journal of Geophysical Research*, *118*. https://doi.org/10.1029/2012JA017916

Ries, G. (1967). Results concerning the sunrise effect of VLF signals propagated over long paths. *Radio Science*, *2*, 531–538.

Rodger, C. J., Clilverd, M. A., & McCormick, R. J. (2003). Significance of lightning-generated whistlers to inner radiation belt electron lifetimes. *Journal of Geophysical Research*, *108*(A12), 1462. https://doi.org/10.1029/2003JA009906

Salut, M. M., Abdullah, M., Graf, K. L., Cohen, M. B., Cotts, B. R. T., & Kumar, S. (2012). Long recovery VLF perturbations associated with lightning discharges. *Journal of Geophysical Research*, *117*, A08311. https://doi.org/10.1029/2012JA017567

Salut, M. M., Cohen, M. B., Ali, M. A. M., Graf, K. L., Cotts, B. R. T., & Kumar, S. (2013). On the relationship between lightning peak current and early VLF perturbations. *Journal of Geophysical Research: Space Physics*, *118*. https://doi.org/10.1002/2013JA019087

Snyder, F. P., & Pappert, R. A. (1969). A parametric study of the VLF mode below anisotropic ionosphere. *Radio Science*, *4*(3), 213–226. https://doi.org/10.1029/RS004i003p00213

Strobel, D. F., Young, T. R., Meier, R. R., Coffey, T. P., & Ali, A. W. (1974). The nighttime ionosphere: E region and lower F region. *Journal of Geophysical Research*, *79*(22), 3171–3178. https://doi.org/10.1029/JA079i022p03171

Thomson, N. R. (1993), Experimental daytime VLF ionospheric parameters, *Journal of Atmospheric and Terrestrial Physics*, *55*, 173–184, doi:https://doi.org/10.1016/0021-9169(93) 90122-F.

Thomson, N. R. (2010). Daytime tropical D region parameters from short path VLF phase and amplitude. *Journal of Geophysical Research*, *115*, A09313. https://doi.org/10.1029/2010JA015355

Thomson, N. R., & Clilverd, M. A. (2001). Solar flare induced ionospheric D region enhancements from VLF amplitude observations. *Journal of Atmospheric and Solar - Terrestrial Physics*, *63*(16), 1729–1737. https://doi.org/10.1016/S1364-6826(01)00048-7

Thomson, N. R., Clilverd, M. A., & McRae, W. M. (2007). Nighttime D region parameters from VLF amplitude and Phase. *Journal of Geophysical Research*, *112*, A07304. https://doi.org/10.1029/2007JA91227

Thomson, N. R., Clilverd, M. A., & Rodger, C. J. (2011). Daytime midlatitude D region parameters at solar minimum from short-path VLF phase and amplitude. *Journal of Geophysical Research*, *116*, A03310. https://doi.org/10.1029/2010JA016248

Thomson, N. R., Clilverd, M. A., & Rodger, C. J. (2014). Low-latitude ionospheric D region dependence on solar zenith angle. *Journal of Geophysical Research*, *119*(8), 6865–6875. https://doi.org/10.1002/2014JA020299

Thomson, N. R., & McRae, W. M. (2009). Nighttime ionospheric D region: Equatorial and nonequatorial. *Journal of Geophysical Research*, *114*, A08305. https://doi.org/10.1029/2008JA014001

Voss, H. D., Walt, M., Imhof, W. L., Mobilia, J., & Inan, U. S. (1998). Satellite observations of lightning-induced electron precipitation. *Journal of Geophysical Research*, *103*, 11,725–11,744.

Wait, J. R. (1957). The attenuation vs. frequency characteristics of VLF waves. *Proceedings of the IRE*, *45*, 768–771.

Wait, J. R. (1962). *Electromagnetic waves in stratified media*. Tarrytown, N. Y.: Pergamon.

Wait, J. R., & Spies, K. P. (1964). Characteristics of the earth-ionosphere waveguide for VLF radio waves, Tech. Note 300, Nat. Burr. Of Stand., Boulder, Colo.